

# Distributed Control of Antenna Array with Formation of UAVs

Stefania Tonetti\* Markus Hehn\*\* Sergei Lupashin\*\*  
Raffaello D'Andrea\*\*

\* *Department of Aerospace Engineering, Politecnico di Milano, Milano, Italy (e-mail: tonetti@aero.polimi.it).*

\*\* *Institute for Dynamic Systems and Control (IDSC), ETH Zurich, Zurich, Switzerland (e-mail: {hehnm,sergeil,rdandrea}@ethz.ch)*

---

**Abstract:** This paper studies the feasibility and the advantages of a distributed control strategy for a linear end-fire antenna array formation with UAVs. We first analyze the sensitivity of different interaction topologies to a low frequency sinusoidal disturbance affecting just one single vehicle, for antenna array sizes of up to 30 elements. The ETH Zurich Flying Machine Arena (FMA) is used as a test case. Then we consider a more realistic case of wind gust acting on all of the antennas. We show that under such conditions the simplified analysis does well at predicting the formation behavior under different distributed and decentralized control strategies.

---

## 1. INTRODUCTION

In recent years there has been an increasing interest in small Unmanned Aerial Vehicles (UAVs) for numerous applications (see for example Chandler et al. [2002], Beard and McLain [2004] and the references therein). UAVs can cover wide spaces and they are popular in military, surveillance and exploration missions, such as Synthetic Aperture Radar (Stiles et al. [2002]), environmental monitoring, pollution control and drag reduction via close formation flight (Wolfe et al. [1996]).

The idea of using a cluster of UAVs as a phased antenna array offers significant potential advantages and remains a popular research topic. Each vehicle in the formation carries a single-element antenna such that together they form an array. Antenna arrays are widely used in communication systems because they have several advantages over a single-element antenna: they increase mobility; they facilitate changing frequencies and direction by reconfiguration; and they can provide higher directivity, higher antenna gain and higher signal to noise ratio on the received signal. One drawback of the UAV antenna array is that the antennas are not rigidly connected; the array is thus sensitive to disturbances caused by wind around the aircraft. Position errors become a significant problem to solve and require an effective control strategy. Control problems associated with autonomous vehicles in formation flight have been investigated: in Wolfe et al. [1996] decentralized controllers are proposed for a formation of five aircraft; in Breheny et al. [2003] the feasibility of using several UAVs to form a phased antenna array is analyzed; in Chandra et al. [2008] linear controllers are proposed to correct for vehicle position errors. In all the works mentioned above the control is totally decentralized, meaning each agent is controlled by a local controller  $C_i$  which accesses only the state of agent  $i$  with no information exchange among the other vehicles. However, for the purpose of formation control, a decentralized control cannot guarantee precise relative distances among the agents. A new kind of control

strategy is therefore needed for multi-agent systems, and distributed control techniques are an attractive option. In a distributed control architecture each agent is equipped with a local controller  $C_i$  which receives information not only on the state of agent  $i$  but also on the state of a subset of other vehicles in the formation. Applications of coordinated control of multiple vehicles has been addressed in many fields and some examples can be found in Kapilal et al. [1999] for microsatellite clusters, in Bender [2002] for automated traffic systems and in Feddema et al. [2002] for mobile robotics.

The main contribution of this paper is to show the feasibility of a distributed control strategy for an antenna array formation with UAVs. We consider a given antenna array design. We control each vehicle's position using a feedback law with the input consisting of the vehicle's individual state plus any available states of the neighbors. We show that in the presence of disturbances, a distributed control strategy can ensure better relative position control than a decentralized one, leading to higher antenna directivity. Extending the results in Tonetti and Murray [2010] on limits in performance for multi-agent systems, different interconnection topologies are studied.

The paper is organized as follows. In Section 2 we summarize principal concepts on antenna arrays and graph theory. In Section 3 we propose the quadcopter and distributed control models. We report simulation and real-world results in Section 4, and present our conclusions in Section 5.

## 2. PRELIMINARIES

### 2.1 Antenna Array Theory

In this section we present a brief introduction to antenna array theory. For a more detailed treatment we refer the reader to Balanis [1997].

An antenna is defined as a device that is able to receive or transmit electromagnetic energy. An antenna may consist of one or more components. A single-element antenna's performance is too limited for some applications. A set of discrete elements, called an antenna array can be used to improve the technical characteristics of a single-element antenna. An antenna array is defined as multiple antennas arranged in space and connected electrically with controlled amplitude  $I$  and phase  $\beta$  to produce a desired directional (higher gain) pattern via constructive interference.

The performance of antennas is characterized by many specific parameters and indices, including: beamwidth, efficiency, side lobe level, null constraints and directivity. We focus mainly on directivity. The directivity  $D$  of an antenna in a given direction  $(\theta, \phi)$  is defined as the ratio of the radiation intensity in the above-mentioned direction to the average radiation intensity and for  $N$  point sources can be expressed as

$$D(\theta, \phi) = \frac{E^2(\theta, \phi)}{\sum_{n=1}^N I_n^2}, \quad (1)$$

where  $\theta$  and  $\phi$  are the polar and azimuthal angles in spherical polar coordinates, respectively (Fig. 1),  $E(\theta, \phi)$  is the magnitude of the electric field and  $I_n$  is the amplitude of the  $n$ th source. The magnitude of the electric field  $E(\theta, \phi)$

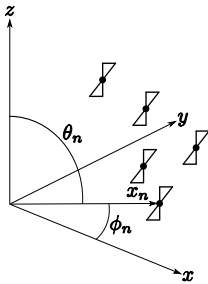


Fig. 1. Geometry of an antenna array

of  $N$  isotropic point sources with the same configuration is proportional to

$$E(\theta, \phi) \propto \left| \sum_{n=1}^N I_n e^{j(2\pi x_n \cos \xi_n + \beta_n)} \right|, \quad (2)$$

where  $\beta_n$  is the phase of the  $n$ th source,  $x_n$  is the distance of the  $n$ th source point from the origin measured in wavelengths and

$$\cos \xi_n = \sin \theta \sin \theta_n \cos(\phi - \phi_n) + \cos \theta \cos \theta_n. \quad (3)$$

The directivity is a measure of the concentration of the radiated power in a particular direction and therefore, in order to ensure good performance, the antenna directivity should be as large as possible in the direction of the receiver.

## 2.2 Graph Theory

In this section we summarize some of the key concepts from graph theory that are used in the paper. A more detailed presentation of graph theory can be found in Tutte [2005].

A directed graph  $\mathcal{G}$  is a set of nodes  $V$  and a set of arcs  $A \subset V^2$  whose elements  $a = (u, v) \in A$  characterize

the relation between distinct pairs of nodes  $u, v \in V$ . A graph is undirected if for every arc  $a = (u, v) \in A$  there exists  $a = (v, u) \in A$ . For an arc  $(u, v)$  we call  $u$  the tail and  $v$  the head. The in(out) degree of a node  $v$  is the number of arcs with  $v$  as its head (tail). A directed path in a graph is a sequence of nodes such that from each of its nodes there is an arc to the next node in the sequence. A directed graph is "strongly connected" if there is a directed path from each node in the graph to every other node. A complete directed graph is a graph where each pair of nodes has an arc connecting them. A simple cycle is a closed path that is self-avoiding (does not revisit nodes, other than the first). A (un)directed cycle graph is an undirected graph that consists of a single (un)directed cycle which visits each node exactly once. The structure of a graph can be described in matrix form. The normalized Laplacian matrix  $\mathcal{L}$  of a directed graph  $\mathcal{G}$  is a square matrix of size  $|V|$ , defined by  $\mathcal{L}_{ij} = 1$  if  $i = j$ ,  $\mathcal{L}_{ij} = 1/d_i$  if  $(i, j) \in A$ , where  $d_i$  is the outdegree of the  $i$ th vertex,  $\mathcal{L}_{ij} = 0$  otherwise.

## 3. DISTRIBUTED CONTROL DESIGN

### 3.1 Quadcopter Model

We consider a 2D model of a quadcopter moving in the  $xz$ -plane (Fig. 2). Out-of-plane dynamics are decoupled

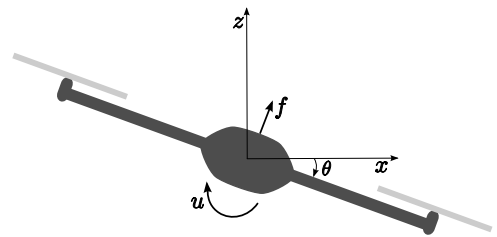


Fig. 2. Simplified 2D model of a quadcopter and coordinate system

and stabilized separately. The model is:

$$\begin{aligned} \ddot{x}(t) &= f(t) \sin \theta(t) \\ \ddot{z}(t) &= f(t) \cos \theta(t) - g \\ \dot{\theta}(t) &= u(t), \end{aligned} \quad (4)$$

where  $f(t)$  is the collective normalized thrust in  $m/s^2$ ,  $\theta(t)$  is the pitch angle,  $g$  is the gravitational acceleration and  $u(t)$  is the pitch rate in  $rad/s$ .

Position control keeps the quadcopter over a desired point. The actual commands that are sent to the vehicle are angle rates and collective normalized thrust. Because of the very fast response time to variations in the rotational rate, the pitch rate is assumed as control input ignoring dynamics and delay. The quadcopter's entire state is assumed to be known thorough an estimator. Assuming constant height  $z_d$ , horizontal motion is achieved by pitching the quadcopter in response to a deviation from the  $x_d$  reference. We assume near-hover operation, which implies small pitch angles. It is therefore possible to linearize the dynamics about the hover operating point, with only small linearization errors. The linear approximation about hover for the  $x$ -dynamics results in a triple integrator:

$$\ddot{x}(t) = g\dot{\theta}(t) = gu(t), \quad (5)$$

and it relates the position  $x(t)$  to the angle rate input  $u(t)$ . The feedback term to correct for errors is

$u(t) = k_2(\ddot{x}_d(t) - \ddot{x}(t)) + k_1(\dot{x}_d(t) - \dot{x}(t)) + k_0(x_d(t) - x(t))$ , where  $k_2$ ,  $k_1$  and  $k_0$  are control parameters acting on the acceleration, velocity and position errors, respectively. In order not to have derivatives as control inputs, we consider an inner loop to stabilize velocity and acceleration, and an outer loop to stabilize position, as shown in Fig. 3, where

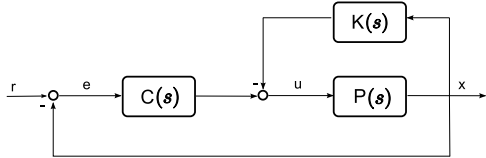


Fig. 3. Block diagram of quadcopter's  $x$ -dynamics feedback control

$P(s) = g/s^3$ ,  $K(s) = k_1s + k_2s^2$  and  $C(s) = k_0$ . With this scheme the transfer function from reference  $r$  to output  $x$  is

$$L(s) = k_0/(s^3 + k_2s^2 + k_1s), \quad (6)$$

and the sensitivity transfer function from reference  $r$  to error  $e$  is

$$S(s) = \frac{s^3 + k_2s^2 + k_1s}{s^3 + k_2s^2 + k_1s + k_0}. \quad (7)$$

Choosing as control parameters  $k_0 = 1.90 \text{ m}^{-1}\text{s}^{-1}$ ,  $k_1 = 1.81 \text{ m}^{-1}$ ,  $k_2 = 0.56 \text{ s m}^{-1}$ , at low frequency  $L(s)$  has large magnitude while  $|S(s)|$  is near zero, leading to good load disturbance rejection and reference tracking. At high frequency the loop gain is small to avoid amplifying measurement noise. The system cut-off frequency is  $\omega_c = 1.05$ . The sensitivity function's peak value is 1.38. The controller stabilizes the quadcopter's dynamics with gain margin of 5.3 and  $70^\circ$  of phase margin. Our model is a linear approximation and the real system is affected by delays on sending commands. A more realistic model should at least include this latency, with a realistic value of  $\tau = 40 \text{ ms}$ . However the system has a delay margin of 1.2 s and therefore the latency can be ignored.

### 3.2 Distributed Control

Since in a vehicle-based antenna array the elements are not attached to a rigid structure (which would ensure nearly perfect positioning), a precise and robust control scheme is needed to correct for deviations from the ideal position due to perturbations, such as wind. Good relative positioning is important in order to maximize directivity in a desired direction.

For simplicity in design and fabrication, the elements of an array are assumed to be identical and parallel. In this paper we consider linear end-fire arrays of identical elements. That means antenna elements are arranged in a straight line, the receiver is along the direction of this line and the direction of the main lobe maximum is within the plane containing the antenna. Specifically, we deal with a phased array, i.e., an array of identical elements fed with current sources of identical amplitude, but which achieves a given pattern by changing the phase of the individual array elements  $\beta_n$ . Phased arrays can be used to steer the main beam of the antenna without physically

moving the antenna. It must be stressed, however, that phase correction works well only if position errors are small because the correction can change the relationship between element current and radiated power. Another important characteristic is the width of the beam, which depends more on the array formation than on the phase. In a given beam, width is dependent on the spacing between the elements. Therefore we focus mainly on keeping the desired formation, in order to reduce as much as possible the phase shifting correction needed for inevitable position errors.

Consider a linear end-fire array of  $N$  isotropic sources placed along the  $x$ -axis at distances  $x_1 < x_2 < \dots < x_N$ . It can be proved that deviations from the nominal position in  $y$  and  $z$  are quadratic or higher order errors in the expression of the directivity because motion in these directions is perpendicular to the receiver direction (Chandra et al. [2008]). Therefore they can be controlled in a decentralized way, while deviations in  $x$ , i.e. the relative distance between vehicles on a straight line, are controlled through a distributed approach. We consider the multi-agent feedback system in Fig. 4, where the normalized Laplacian matrix  $\mathcal{L}$  represents the interaction topology;  $\hat{P}(s)$ ,  $\hat{C}(s)$  and  $\hat{K}(s)$  represent matrices with  $P(s)$ ,  $C(s)$  and  $K(s)$  repeated  $N$  times along the diagonal, respectively;  $\mathbf{r} \in \mathbb{R}^N$  is the vector of the reference signals of each agent;  $\mathbf{e} \in \mathbb{R}^N$  are the errors between  $\mathbf{r}$  and the process outputs  $\mathbf{x} \in \mathbb{R}^N$ ;  $\mathbf{u} \in \mathbb{R}^N$  is the control signal vector;  $\mathbf{d} \in \mathbb{R}^N$  is the disturbance acting on each vehicle. From the point of view of formation stability, it is worth

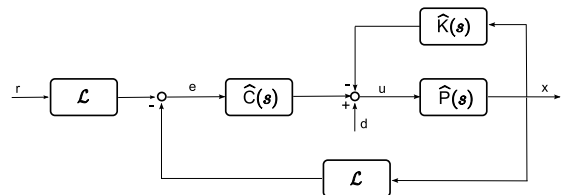


Fig. 4. Block diagram of the antenna array feedback control along  $x$

noting that the Nyquist plot of the open loop transfer function lies entirely in the half plane  $x > -0.5$ . This is important because all the relative formation critical points lie in the half plane  $x \leq -0.5$  (Fax and Murray [2004]) and therefore the relative formation dynamics are stable for every possible interaction topology.

## 4. SIMULATION AND EXPERIMENTAL RESULTS

### 4.1 Model Validation

In this section a validation of the multi-agent feedback control model presented in Section 3 is given.

The ETH Zurich Flying Machine Arena (FMA) is an experimental platform for validating theoretical advances in control of small flying vehicles. The overall organization of the system is similar to How et al. [2008]. The arena of  $10\text{m} \times 10\text{m} \times 10\text{m}$  is equipped with a 8-camera Vicon motion capture system to achieve marker localization at 200 Hz with millimeter accuracy. Each quadcopter carries a unique arrangement of three such markers so that

the Vicon system can determine each vehicle's position and attitude at each frame with a latency of about 20 ms. For a more detailed description of the platform the reader is referred to Lupashin et al. [2010], Schöllig et al. [2010], Hehn and D'Andrea [2011]. The flying vehicles currently used in the Arena are highly modified Ascending Technologies X3D 'Hummingbird' quadcopters.

For the purpose of this paper, all the vehicles' pose data are received by the same computer, which computationally simulates the distributed control. The model validation is performed with 3 quadcopters controlled with a leader-follower topology depicted in Fig. 5, where vehicle 1 is the leader, while vehicles 2 and 3 are followers. Each follower can sense only the agent in front of it. The nominal

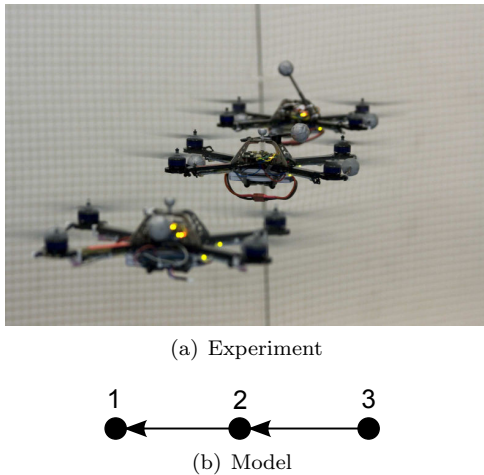


Fig. 5. Leader-Follower topology

positions are  $x_1 = 0$  m,  $x_2 = 1$  m and  $x_3 = 2$  m. A sinusoidal movement with amplitude  $A = 0.2$  m and frequency  $\omega = 0.1$  rad/s is commanded to the leader and the followers adjust their own position in order to keep the desired relative distance of 1 m with respect to the vehicle in front. The comparison between model and reality (see Fig. 6) shows that, even if the model is linear and it does not take into account measurement noise and other disturbances due to environment, the real system behavior is predicted with reasonable accuracy, with position errors of at most 3% of the distance between two vehicles. From

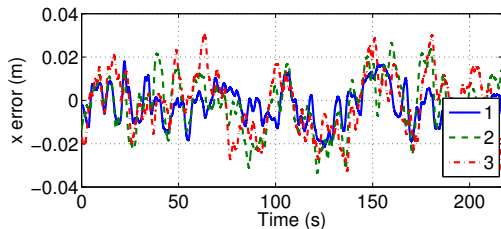


Fig. 6. Time history of the  $x$  errors for the three quadrotors

now on all the results will be produced in simulation using the validated linear multi-agent feedback control model presented in Section 3.

#### 4.2 Antenna Array Objective Function

Suppose the nominal design of the formation to be given, and  $0 = x_1 < x_2 < \dots < x_N$  to be the ideal positions

within the array with respect to the formation origin, arbitrarily chosen as the first vehicle in the formation. Let  $x'_n$  ( $n = 1, \dots, N$ ) be the measured relative positions of the vehicles with respect to the formation origin, with  $x'_1 = 0$  by construction. In order to maximize directivity, for the phase nominal design we choose  $\beta_n = -2\pi x_n \cos \phi_0$ . Suppose we want to maximize the directivity in the direction  $\theta = \frac{\pi}{2}$ ,  $\phi_0 = 0$ , the magnitude of the electric field expressed in (2) becomes

$$E\left(\frac{\pi}{2}, 0\right) \propto \left| \sum_{n=1}^N I_n e^{j2\pi\delta_n} \right|, \quad (8)$$

where  $\delta_n = x'_n - x_n$  is the position error in wavelength of the  $n$ th element with respect to the formation origin. Substituting equation (8) in the expression of directivity (1) and assuming antennas are fed with the same current  $I_n = I \forall n = 1, \dots, N$ , we state the objective function in presence of relative position errors as follows:

$$D\left(\frac{\pi}{2}, 0\right) = \frac{1}{N} \left[ \left( \sum_{n=1}^N \cos(2\pi\delta_n) \right)^2 + \left( \sum_{n=1}^N \sin(2\pi\delta_n) \right)^2 \right]. \quad (9)$$

The objective function defined above takes its maximum value of  $N$  when all the errors are equal to zero, and it is used to evaluate performances of different control strategies.

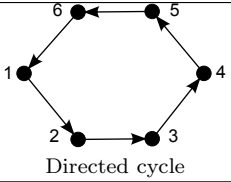
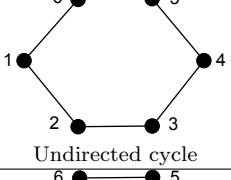
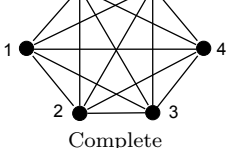
#### 4.3 Sensitivity to a Single-Agent Disturbance

In order to simplify the analysis, this section presents a comparison on minimum directivity achievable applying decentralized and distributed control strategy for station-keeping in presence of a disturbance acting on a single agent. Starting from results obtained in Tonetti and Murray [2010] it is possible to predict the array behavior in the presence of a low frequency sinusoidal disturbance acting on one agent by simply evaluating the appropriate network sensitivity functions at that frequency.

A sinusoidal perturbation along  $x$  with frequency  $\omega_d \ll \omega_c$  is introduced in one element. The output position of the moving quadcopter results in a sinusoidal movement with amplitude  $A$ . This is considered the reference to follow for all the other vehicles, in order to keep the desired relative distances. Referring to Breheny et al. [2003], assume each quadcopter is equipped with an antenna operating at 150 MHz, with wavelength of approximately 2 m at that frequency. The nominal relative distance between neighboring elements is assumed to be uniform and equal to 0.5 wavelengths.

If a decentralized controller is used, i.e., each agent adjusts its position only according to its own state, the agent perturbed moves sinusoidally with  $x = A \sin(\omega_d t)$ , while the others simply keep their absolute position. What we are looking for is a strongly connected topology, meaning that each vehicle can sense every other vehicle because every pair of nodes is connected by a directed path. From Tonetti and Murray [2010] it is known that there are limitations on multi-agent systems performance. If a strongly connected graph is used and the task is to keep as small as possible all the relative distances, the best we can achieve is a low frequency disturbance attenuation factor of  $1/N$  for all the agents, with topologies that equally

Table 1. Graph topologies and relative Laplacian matrices used to control the linear end-fire array

Topology	Laplacian matrix
 <p>Directed cycle</p>	$\mathcal{L}_{ij} = \begin{cases} 1 & \text{if } i = j \\ -1 & \text{if } (i, j) \in A \\ 0 & \text{otherwise} \end{cases}$
 <p>Undirected cycle</p>	$\mathcal{L}_{ij} = \begin{cases} 1 & \text{if } i = j \\ -\frac{1}{2} & \text{if } (i, j) \in A \\ 0 & \text{otherwise} \end{cases}$
 <p>Complete</p>	$\mathcal{L}_{ij} = \begin{cases} 1 & \text{if } i = j \\ -\frac{1}{N-1} & \text{otherwise} \end{cases}$

distribute cycles on the nodes. Notice that  $\delta_n$  assumes in general different meaning from the error  $e_n$  in Fig. 4:  $\delta_n = x'_n - x_n$ , while  $e_n = \mathcal{L}(x_n - x'_n)$ . The latter depends on the interaction topology through the Laplacian matrix  $\mathcal{L}$ . However, the two errors can be easily related through some algebraic computations. Examples for a 6-element antenna array of the interconnection topologies and corresponding normalized Laplacian matrices used in the simulation are listed in Table 1. If the control is decentralized  $\mathcal{L} = I_{(N)}$ . It should be stressed that diagrams in Table 1 capture the interconnection topology, while the vehicle formation is arranged in a straight line to form a linear end-fire array. Since the disturbance is sinusoidal, directivity also assumes periodic values in time. To evaluate performance, only the minimum directivity value along  $(\frac{\pi}{2}, 0)$  is considered, and in Fig. 7 it is shown for different array sizes, normalized to the number of agents. From Fig. 7 it is clear that for

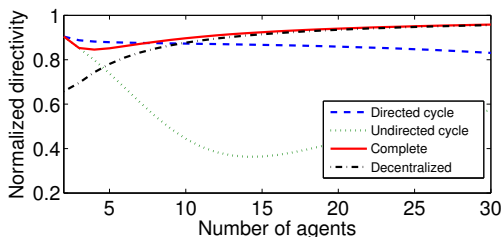


Fig. 7. Minimum guaranteed directivity: comparison between different control strategies

$N < 8$  a directed cycle is the best choice, while for  $N \geq 8$  the complete directed graph ensures higher directivity than a decentralized one. This is explained looking at the relative errors  $\delta_n$  for the two topologies: in a directed cycle the relative error depends on the length of the path from the quadcopter  $n$  to the perturbed agent  $\delta_n = An/N$ , while a complete graph ensures the same relative error equal to  $\delta_n = A(N-1)/N$ , for all the agents. However, as the number of antennas increases, the behavior of the distributed control with complete graph topology tends

asymptotically to the decentralized one. For example, with 20 agents the improvement in directivity using a distributed strategy compared to a decentralized one is about 0.6% and it decreases to 0.3% for 30 antennas. This is because of how  $\mathcal{L}$  is defined: when  $N$  grows, the control weight on the other agents position becomes smaller and smaller, tending to zero for  $N$  going to infinity, and therefore quadcopters tend to behave like a single agent. As expected in the case of decentralized control, single agent error becomes less significant and the normalized directivity becomes higher as the number of antennas is increased. An undirected cycle topology never guarantees a good performance.

#### 4.4 Sensitivity to Wind Gusts

In this section we generalize results obtained previously to a more realistic case of disturbance caused by wind gusts.

Wind is the main source of antenna disturbance. The total wind velocity is a combination of a mean velocity and a gust velocity. The gust component can be modeled as a random process with zero mean and a spectrum called the Davenport spectrum (Simiu and Scanlan [1978]). Davenport filter is used to shape white noise  $w$  of unit standard deviation into wind gusts. The filter transfer function  $H(s)$  is of fourth order and was obtained in Gawronski et al. [1994].

In our model the wind gusts are applied at the rate input, but the output of Davenport filter is a velocity. Therefore wind gust has to be appropriately filtered with filter  $F(s) = (k_t s)/k_d$  to produce a rate that is added to the rate input of the antenna. First velocity gust is scaled with gain  $k_t$  to obtain wind torque and next the torque is filtered to obtain a rate. Coefficients  $k_t$  and  $k_d$  are torque factor and drive gain, respectively, depending on physical characteristics of the antenna, wind direction and velocity. We study the worst case scenario from the directivity point of view, where wind gusts are directed along the  $x$  axis. We consider wind gust signals  $\tilde{w} = F(s)H(s)w$  colored in time because filtered, but spatially white because uncorrelated from one agent to the other. Disturbance is added to the control law input  $u$  and we compute the normalized directivity obtained with different control strategies. The white noise vector  $\mathbf{w}$  generated for the simulation is the same for all the topologies, in order to better compare results. According to Fig. 7, for 3 antennas we expect single cycle to guarantee the highest directivity and complete graph topology to behave well, while the decentralized control to be the worst. In Fig. 8 we can see that the simplified model in section 4.3 predicts the antenna array behavior with good accuracy. For an antenna array of 16 elements we expect the directed cycle to be the worst choice, while the complete graph and decentralized control to guarantee almost the same directivity, with the complete one to be a little better (see Fig. 9).

## 5. CONCLUSION

In this paper we have shown that, in the case of formation quadcopters, an improvement in antenna array directivity can be achieved by applying a station keeping

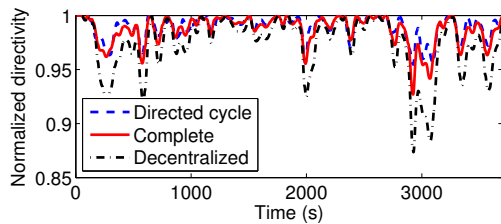


Fig. 8. Normalized directivity for 3 elements antenna array in presence of wind gusts

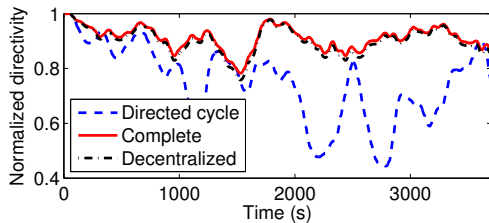


Fig. 9. Normalized directivity for 16 elements antenna array in presence of wind gusts

distributed control, instead of a decentralized one. We have proposed a simplified method to evaluate array performance that satisfactorily predicts the formation behavior even in presence of wind gusts. Even if distributed control always ensures the higher directivity, we can in general conclude that a complete graph topology is indicated if the elements forming the antenna array are limited to a small number, while a decentralized control is indicated for a high number of agents. With mid-sized groups, one must choose between loss in directivity caused by decentralized control, and communication and computational effort needed from the distributed strategy.

The distributed control strategy considered throughout this paper does not take into account errors in absolute position. It is, however, important to keep the formation precisely oriented towards the receiver. In order to overcome this issue a mixed absolute/relative control should be implemented, where knowledge on global coordinates is available to the entire formation. Another problem not addressed in our work is the single element orientation error. Directivity is influenced only by relative position errors if all the elements in the formation are identically oriented. Wind gusts and the control actions change antennas' attitude, causing a decreasing in the antenna array directivity. In the present work the information exchange between UAVs is computationally simulated. In a real world implementation the onboard sensors will provide less accurate position measurements, but we expect that reduction in system performance will affect both distributed and decentralized control.

## REFERENCES

C. A. Balanis. *Antenna theory*. John Wiley & Sons, New York, 1997.

R. W. Beard and T. W. McLain. Multiple UAV cooperative search under collision avoidance and limited range communication constraints. In *Proceedings of the 42nd IEEE Conference on Decision and Control*, volume 1, pages 25–30. IEEE, 2004.

J. G. Bender. An overview of systems studies of automated highway systems. *IEEE Transactions on Vehicular Technology*, 40(1):82–99, 2002.

S. H. Breheny, R. D'Andrea, and J. C. Miller. Using Airborne Vehicle-Based Antenna Arrays to Improve Communications with UAV Clusters. In *In Proceedings of 42nd IEEE Conference on Decision and Control*, volume 4, 2003.

P. R. Chandler, M. Pachter, D. Swaroop, J. M. Fowler, J. K. Howlett, S. Rasmussen, C. Schumacher, and K. Nygard. Complexity in UAV cooperative control. In *Proceedings of the American Control Conference*, volume 3, pages 1831–1836. IEEE, 2002.

R. S. Chandra, S. H. Breheny, and R. D'Andrea. Antenna array synthesis with clusters of unmanned aerial vehicles. *Automatica*, 44(8):1976–1984, 2008.

J. A. Fax and R. M. Murray. Information flow and cooperative control of vehicle formations. *IEEE Transactions on Automatic Control*, 49(9):1465–1476, 2004.

J. T. Feddema, C. Lewis, and D. A. Schoenwald. Decentralized control of cooperative robotic vehicles: theory and application. *IEEE Transactions on Robotics and Automation*, 18(5):852–864, 2002.

W. Gawronski, B. Bienkiewicz, and R. E. Hill. Wind-induced dynamics of a deep space network antenna. *Journal of Sound and Vibration*, 178(1):67–77, 1994.

M. Hehn and R. D'Andrea. A Flying Inverted Pendulum. In *IEEE International Conference on Robotics and Automation*. (accepted for publication), 2011.

J. P. How, B. Bethke, A. Frank, D. Dale, and J. Vian. Real-time indoor autonomous vehicle test environment. *IEEE control systems*, 28(2):51–64, 2008.

V. Kapilal, A. G. Sparks, J. M. Buffington, and Q. Yan. Spacecraft formation flying: Dynamics and control. In *American Control Conference, 1999. Proceedings of the 1999*, volume 6, 1999.

S. Lupashin, A. Schöllig, M. Sherback, and R. D'Andrea. A Simple Learning Strategy for High-Speed Quadcopter Multi-Flips. In *2010 IEEE International Conference on Robotics and Automation (ICRA), Proceedings*, 2010.

A. Schöllig, F. Augugliaro, and R. D'Andrea. A platform for dance performances with multiple quadcopters. In *Proceedings of the IEEE/RSJ International Conference on Intelligent Robots and Systems – Workshop on Robots and Musical Expressions*, pages 1–8, 2010.

E. Simiu and R. H. Scanlan. *Wind effects on structures: an introduction to wind engineering*. Wiley New York, 1978.

J. Stiles, N. Goodman, and S.C. Lin. Performance and processing of SAR satellite clusters. In *In Proceedings of Geoscience and Remote Sensing Symposium*, volume 2, pages 883–885. IEEE, 2002.

S. Tonetti and R. M. Murray. Limits on the network sensitivity function for homogeneous multi-agent systems on a graph. In *American Control Conference (ACC), 2010*, pages 3217–3222. IEEE, 2010.

W. T. Tutte. *Graph Theory*. Cambridge University Press, 2005.

J. D. Wolfe, D. F. Chichka, and J. L. Speyer. Decentralized controllers for unmanned aerial vehicle formation flight. *American Institute of Aeronautics and Astronautics*, 96:3933, 1996.